Rapid Sampling of Products During Coal Mine Explosions

RONALD S. CONTI, ISAAC A. ZLOCHOWER and MICHAEL J. SAPKO

Abstract—This paper describes a U.S. Bureau of Mines investigation of large-scale coal dust explosions in an experimental mine using a high speed electropneumatic mechanism for the rapid grab-sampling of gases and dusts. This technique enables the monitoring of pyrolysis and charring in fuel dust particles, and the collection of gaseous combustion products, in both large and small-scale explosions. Data obtained from full-scale dust explosion tests at the Bureau of Mines Lake Lynn Test facility show the following: Rapid sampling appears to "freeze" the burned gas compositions at the flame temperature values. Gas samples taken entirely in the flame zone consist of pyrolysis and combustion products with very low residual oxygen. The particles collected in the flame zone show signs of extensive pyrolysis and charring. Measurements of gas concentrations and particle flame temperatures suggest that char burning may have occurred in the flame zone.

INTRODUCTION

Coal dust explosion research has been conducted for many years at the Bureau of Mines to gain an understanding of the requirements for ignition, propagation, and inhibition of dust explosions. Considerable technical and practical information has been gained from this research, which was used in establishing the present safety standards in the coal mining industry. Nonetheless, dust explosion studies in experimental mines continues to be predominantly empirical due to the absence of a detailed theoretical understanding of the initiation and propagation of combusion waves in mine configurations. Some of the difficulty in developing a theoretical basis is associated with the limitation of the experimental techniques for studying the chemical aspects of full-scale mine explosion processes. This report describes a rapid (grab) sampling system (Conti *et al.*, 1988) for collecting small samples of gases and dusts from the rapidly moving flame front and hot gas zone. This system should promote the collection of accurate chemical data and help expand our knowledge of the flammability behavior of dusts, gases, and inhibitors, which is essential for a realistic appraisal of the explosion hazards involved in coal mining.

EXPERIMENTAL SAMPLING SYSTEM

An array of novel collector devices is used. Each device consists of an aluminum housing which incorporates two pre-evacuated glass vials with rubber septums. Upon actuation, the sampling probe needle is forced through the septum with a pressurized air pulse, filling the tube with gas and dust from the mine explosion. After a predetermined time, the sample probe needle is retracted by a second high pressure air pulse to its normal (quiescent) state, allowing the sampling tube to reseal. The onset and duration of sampling are independently variable and controlled by a time-delay relay package.

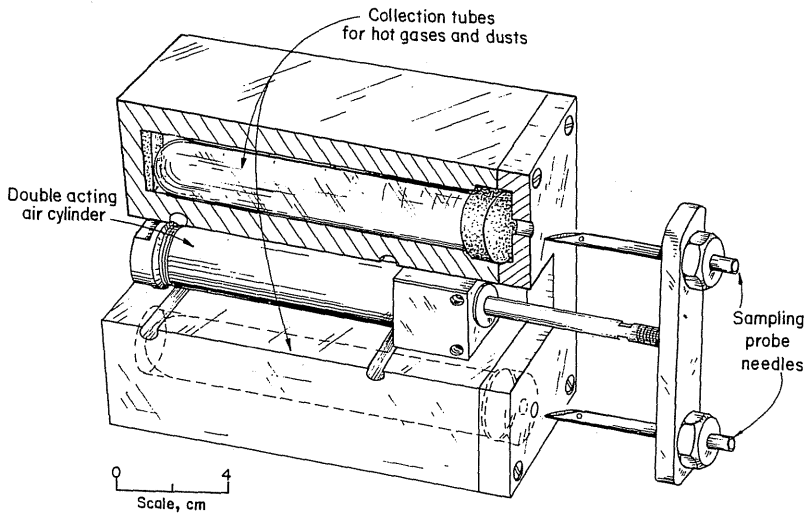

FIGURE 1 Perspective view of mine scale version of rapid-sampling system mechanism.

The mechanical device used to obtain rapid gas and dust grab samples is similar in concept to the previously reported laboratory (Conti *et al.*, 1983) version. In the previous version, however, the probe needles were fixed to the laboratory chamber, and the sealed evacuated tubes were air driven into and out of the needles. In the mine version, the tubes are fixed and the needles move with the piston. The current version is shown in a sectional perspective in Figure 1. The main components of the system are an electropneumatic, double-acting air cylinder to power the sampling system, a piston section to which the sampling probe needles are attached, and the housing for the evacuated glass collection tubes. The 11-gauge (2.39 mm i.d.) hypodermic (sampling probe) needles used are modified by plugging the beveled point and drilling a 1.6 mm hole through the side to minimize septum tearing and core boring by the needle. The sampling system is shown in more detail in Figure 2. The main body is essentially a rectangular aluminum housing with two cylindrical cavities that contain the 30 cc glass collection tubes. The housing cover serves a three-fold purpose, it allows access to the collection tubes, holds the sealed collection tubes in place, and serves as a guide for the sampling probe needles. The two sampling probe needles are mounted on a support bar, which is attached to the piston rod of the double-acting air cylinder. When the system is in the activated state shown in Figure 2, the combustion products are drawn into the evacuated collection tubes. When the preset sampling time is reached, the probe needle returns to its initial position or quiescent state, allowing the rubber septum of the collection tubes to reseal. This predetermined sampling time is controlled by a series of time-delay relays that send electrical pulses to a high speed, direct-solenoid-actuated valve. The initial pulse directs high-pressure (150 psi) air or N_2 from the solenoid valve to a port of the double-acting air cylinders, which forces the sampling probe needles forward into the collection tubes. A similar pulse applied to the opposite port of the double-acting air cylinder returns the sampling probe assembly to its quiescent state, thus completing the sample cycle. After the experiments, the sampling probe needles are removed from the support bar and cleaned. The housing cover is unfastened and the collection tubes are removed for a complete analysis. The use of a number of test devices mounted on a post securely

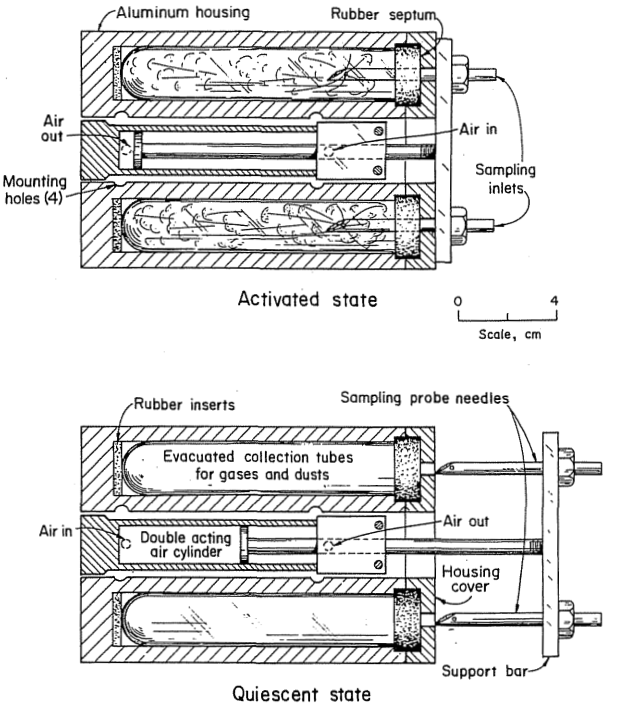

FIGURE 2 Cross-sectional view of rapid-sampling device, in the quiescent and activated states.

fastened to the floor and roof permits the collection of samples at different sampling times and intervals. In principle, the background gas and dust concentration can be obtained before flame arrival, while a brief sampling at flame arrival will give the conditions at the flame front. The contents of the collection tubes are used for duplicate gas analysis, or one is used for gas analyses and the other for microscopic (SEM) analysis of the dust residue.

There are several advantages of this system over previous sampling systems. Sampling starts when the forward stroke of the sampling probe needle penetrates the rubber septum of the sampling tube. The length of sample time and amount of sample are controlled by the time difference in the forward stroke and return stroke of the sampling probe needle. The sample time relative to the combustion process can be measured exactly by observing the sampling probe movement with optical sensors. In previous systems, one monitored the current to the solenoid valves to indicate the approximate start of the sample. The difference between the electrical time, as indicated by the current rise in the solenoid valve, and the actual movement of the sampling probe needle obtained by the optical sensors is about 20 ms. The times reported in this paper are the actual sample times as measured by the movement of the sampling probe needle, using an optical sensor.

LAKE LYNN EXPERIMENTAL MINE

The studies were conducted with the sampling system installed in the D-drift of the Lake Lynn Experimental Mine. The Lake Lynn Laboratory, formerly a limestone mine, is now a multipurpose mining research laboratory operated by the Bureau of

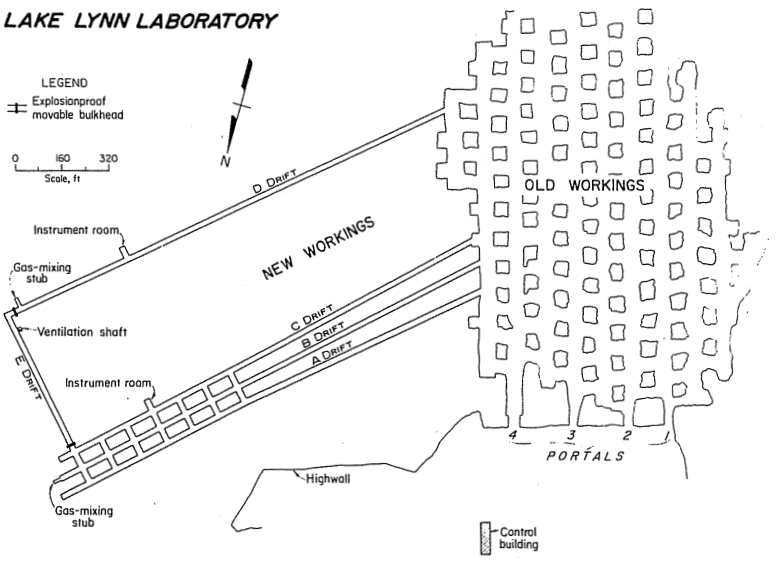

FIGURE 3 Plan view of the Lake Lynn Experimental Mine.

Mines (Mattes *et al.*, 1983). The underground layout of Lake Lynn (shown in Figure 3), allows full-scale research of explosion propagation and suppression as encountered in modern U.S. coal mining. A plan view of the face area in D-drift is illustrated in Figure 4 and shows the configuration for a single entry dust explosion. The average dimensions are 2.1 and 5.8 meters for an average cross-sectional area of 12 m^2.

Instrumentation to monitor pressure development, dust concentration (Conti *et al.*, 1982; Cashdollar *et al.*, 1981), and flame arrival times is provided at 10 stations along 229 meters of the entry, starting at the bulkhead. Flame temperatures are monitored with 3 wavelength pyrometers at several stations. A detailed descrption of the physical arrangement and instrumentation for dust explosion studies at the Lake Lynn Experimental Mine has been published (Sapko *et al.*, 1987; Weiss *et al.*, 1988). A flame

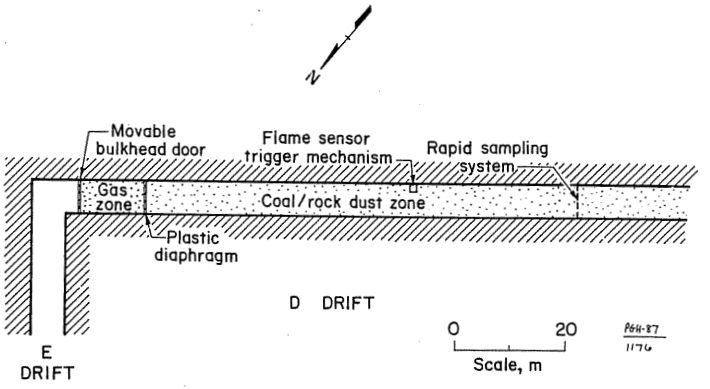

FIGURE 4 Plan view of face area in D-drift showing the configuration of a nominal dust loading for a single entry.

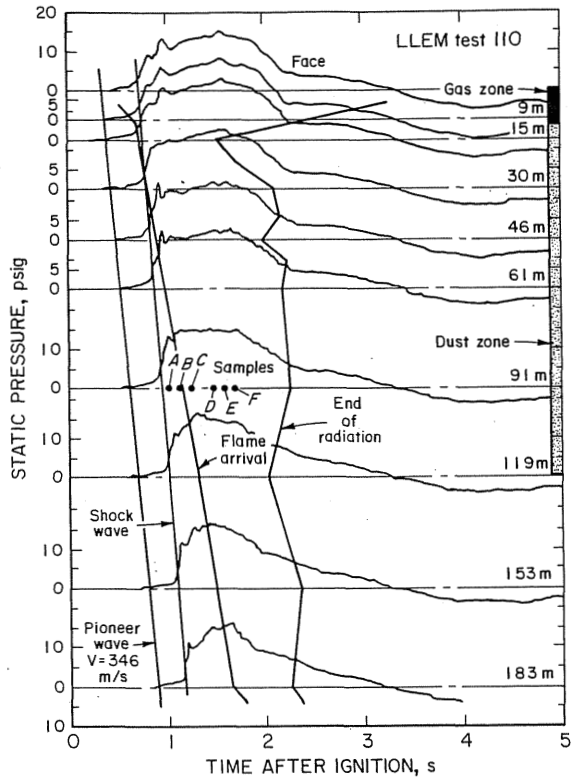

FIGURE 5 Wave diagram of single-entry coal dust, 65% rock dust explosion: LLEM (test 110) D-drift.

sensor trigger device (Liebman *et al.*, 1979a,b) is used to activate the time-delay relays and to control the sampling sequence at the station 30 m further downstream. The device was designed to activate the relays after the initial shock wave has passed and flame radiation has reached the sensor station.

A flammable mixture of methane and air, typically 10% CH_4, is formed by introducing CH_4 in the gas zone and stirring to provide a uniform mixture. Electrically activated pyrotechnic igniters are used to produce the methane explosions in the gas zone. In most experiments, a mixture of 65% rock dust and 35% pulverized (PPC) Pittsburgh seam coal (80%–200 mesh), is spread equally on the floor and on roof shelves in the dust zone to provide a nominal PPC dust concentration near 200 g/m^3, and a total nominal dust concentration of 370 g/m^3 if the dust were uniformly dispersed throughout the dust zone volume by the methane-air explosion. In some experiments, pure PPC is placed only on the shelves to give a nominal concentration near 60 g/m^3 in the dust zone. The flammable dust mixture is dispersed and ignited by the methane-air explosion causing rapid flame propagation down the entry.

The series of explosions involving coal dust mixtures that is described here consisted of a 107 m dust zone containing 60 or 65% pulverized limestone at a nominal PPC concentration of 200g/m^2, that was ignited by a 12 m gas zone consisting of a 10.3% methane-air mixture. Figure 5 is a wave diagram of one such explosion. It plots the change in static pressure with time at the various stations, and includes data on sampling times as well as flame arrival and decay.

The complete sampling system set-up at one of the monitoring stations consists of

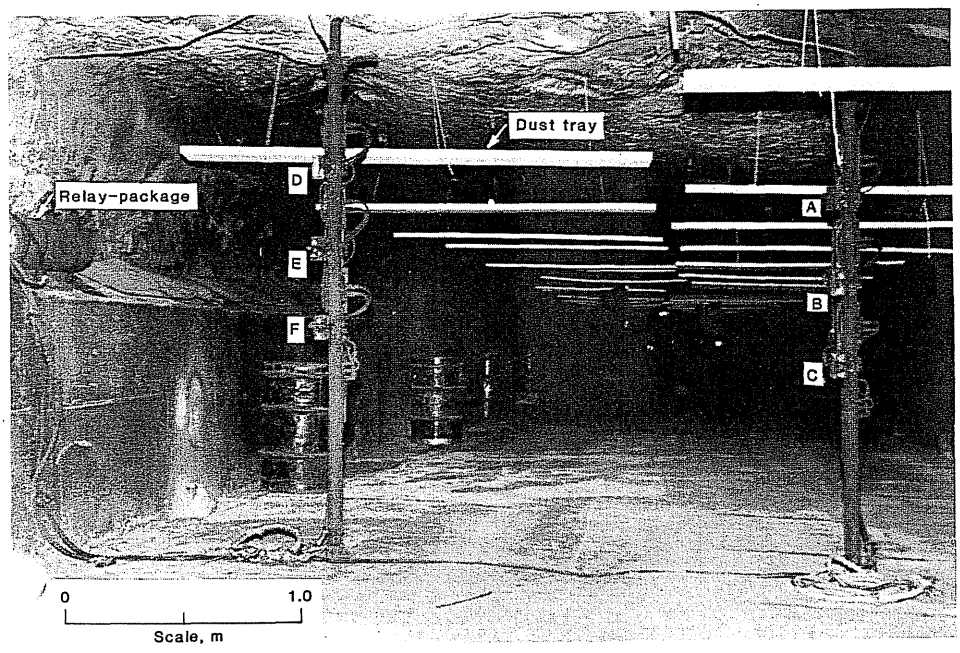

FIGURE 6 Photo of complete sampling system installed in D-drift.

six sampling devices mounted on two vertical stands. The two stands were mounted vertically 91 meters from the face and secured to the mine floor and roof by bolts. The photo in Figure 6 is a cross sectional view of D-drift and shows the sampling system, including the relay control package. The roof shelves or dust trays are in place as are the dust barrels. The latter are removed once their contents are spread out on the floor and shelves of the dust zone.

A sampling cycle comprising the six samplings in a typical test is shown in Figure 7. It indicates when the sampling device is activated and when the device returns to its quiescent state. The shaded portion represents the time in flame or, correspondingly, the length of the flame zone. The numbers at the top of each cycle boundary, indicate the distance between the sampling station and the leading edge of the flame. Thus, Sample B in LLEM-110 was taken starting 7 m ahead of the flame front and concluding 16 m behind the front, but still in the flame zone.

PARTICLE COLLECTION

Particle collection data of the sampling system in test LLEM-110, which featured the timing sequences shown in Figure 7, are presented in Table I. The starting time, t_s, of each sampling device is measured with respect to the initiation of the explosion. The total sample time is Δ_t and t_f is the duration of sampling of the burned gases behind the flame front. The residue (m_c) collected for each sample was weighed using a microbalance and then microscopically analyzed. Sample A, taken after the passage of the methane explosion shock front and just prior to flame arrival, shows the largest amount collected. Sample B was drawn before and during the flame, whereas C through F were taken entirely within the flame. The mass sampling rate was taken as the arithmetic average over the injection interval. It is noted that both the amount of

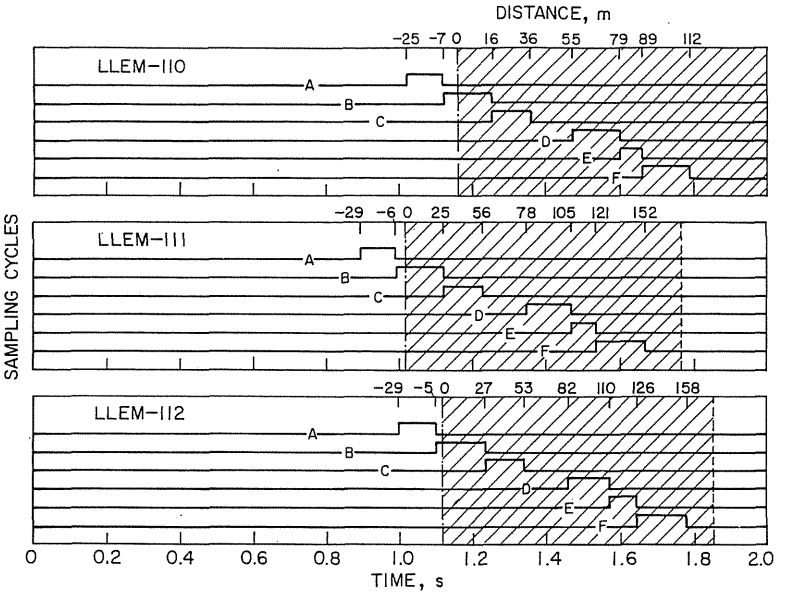

FIGURE 7 Illustration of a typical sampling cycle with respect to flame arrival and the trailing edge of flame for three Lake Lynn experiments.

solids and the collection rate generally decrease with time due, possibly, to char burning and/or coal volatilization. Sampling bias in favor of small particles was not expected in view of previous results with the laboratory version of the rapid sampling device (Conti *et al.*, 1983). No significant change in the trimodal distribution of a mixture of 3 classified coal dusts having mass weighted means of 7.5, 18, and 60 μm was noted after passage through the same needle. The 1.6 mm diameter orifice will, however, prevent passage of any stable agglomerate much larger than 1 mm. Moreover, the fluctuations in local dust concentrations and in flow rate through the needles mitigates against obtaining reliable quantitative information on particle concentration from such mass sampling.

TABLE I
Performance of sampling system; LLEM test No. 110, 35% PPC/65% Rock Dust -200 g/m^3 nominal PPC concentration, flame arrival at 1.161 s.

Sample No.	Sample start t_s, ms	Sample duration Δt, ms	Interval in flame t_f, ms	Mass residue collected m_c, mg	Collection rate r, mg/ms
A	1,041	99	0	50.85	0.51
B	1,140	130	109	15.43	0.12
C	1,270	110	110	8.58	0.08
D	1,490	130	130	7.91	0.06
E	1,620	60	60	4.41	0.07
F	1,680	130	130	6.26	0.05

ELECTRON MICROSCOPE STUDIES

The microscopic structure of coal dust-rock dust mixtures was analyzed by a scanning electron microscope (SEM) system. Ng *et al.* (1983) has provided a detailed description of the SEM and of fire and explosion residues for various dusts. A typical photomicrograph of a 65% rock dust ($CaCO_3$), 35% Pittsburgh pulverized coal (PPC) mixture, both burned and unburned, is shown in Figure 8. The unburned coal particles in Figure 8A collected prior to the explosion have sharp edges and angular features, as opposed to the smooth rounded edges of the burned coal particles shown in Figure 8B that were collected during flame passage. A collection of all the calcium x-ray photons produced during the electron beam scanning of samples 8A and 8B were used to make the x-ray maps in Figures 8C and 8D, respectively. These maps can be used to identify the rock dust particles and how they interact with the coal particles before and after flame passage.

Photomicrographs of samples A–F collected from this explosion (LLEM-110) are shown in Figure 9. After the explosion, the particles are noticeably larger than before the explosion. They exhibit rounded smooth surfaces in contrast to angular and sharp edges of the particles before the explosion. Many of the particles in the explosion show blowholes and bubbly masses, and some have formed cenospheres. This is due to rapid heating of the particles that leads to out-gassing of volatiles which causes the softened coal particle to swell, and eventually leads to the formation of blowholes of various sizes.

GAS ANALYSES

Gas samples were collected both before and after flame arrival at the sampling station, as described above. These were dried and analyzed by gas chromatography for N_2, Ar, O_2, CO_2, CO, H_2, CH_4, C_2H_2, C_2H_4, C_2H_6, C_3H_6, C_3H_8, C_4H_{10}, and C_5H_{12}. Samples collected after ignition and prior to flame arrival gave an average composition which is very close to standard dry air as shown in Table II. The small excess of CO_2 detected together with the small concentrations of CO and CH_4 that were also found are probably due to residual gases from previous explosion.

The confirmation that the test zone atmosphere in front of the flame is basically air is not as obvious as it may seem. Consider that, typically, a 12 m zone from the D-drift bulkhead filled with stoichiometric methane-air is ignited. If the combustion products from the resulting methane explosion are mixed with the remaining air in the 119 m zone to the sampling station, then significant concentrations of CO_2 (1.4%) from the explosion should be detected. The fact that the CO_2 concentration is only increased, on average, from the 0.03% of standard air to 0.09% indicates that longitudinal gas mixing is minimal. The hot burned gas acts primarily as a piston, pushing the coal dust laden air ahead of it. Richmond and Liebman (1975 and 1978) had reached the same conclusion on the basis of explosion measurements made in the experimental mine at Bruceton.

Also shown in Table II is the average composition of the samples collected after flame arrival. These results do not include the few samples whose compositions gave evidence of air dilution (leaking). The average "Flame Zone" composition consists of both coal vapors and their combustion products. The former consists of the hydrocarbon gases (CH_4, C_2H_2, C_2H_4, C_2H_6, C_3H_6, etc.) as well as H_2 and some of the CO and CO_2 produced. The fact that acetylene is the most abundant hydrocarbon after methane is both evidence for the high temperatures produced in the explosion, and

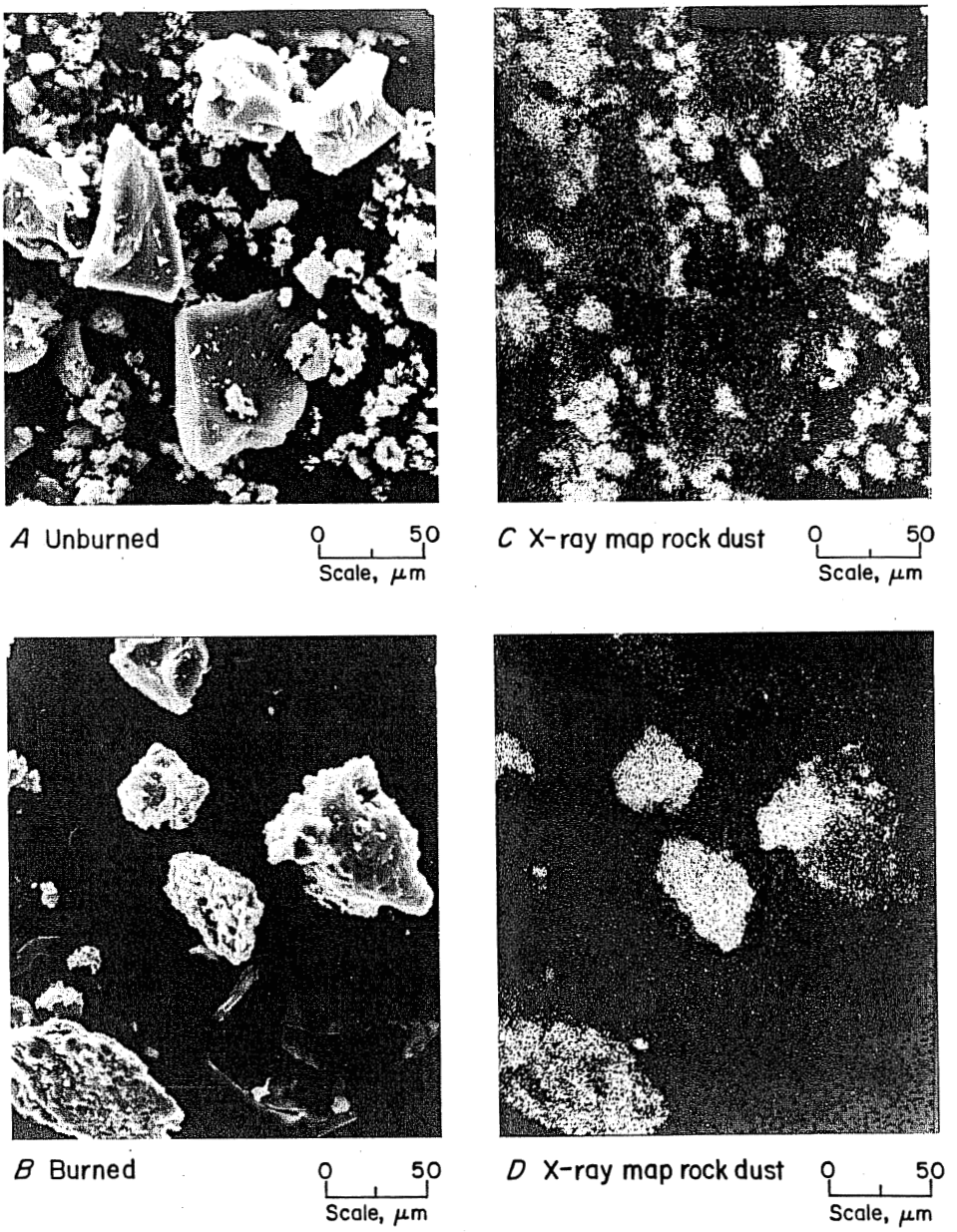

FIGURE 8 Typical SEM photomicrographs of burned and unburned Pittsburgh coal and 65% rock dust particles, X-ray maps made using the calcium line.

the effectiveness of the sampling technique in preserving such an unstable species by means of rapid cooling. Possible contribution, however, to the concentration of the other hydrocarbons by collected particles that continue to devolatilize cannot be ruled out at this point.

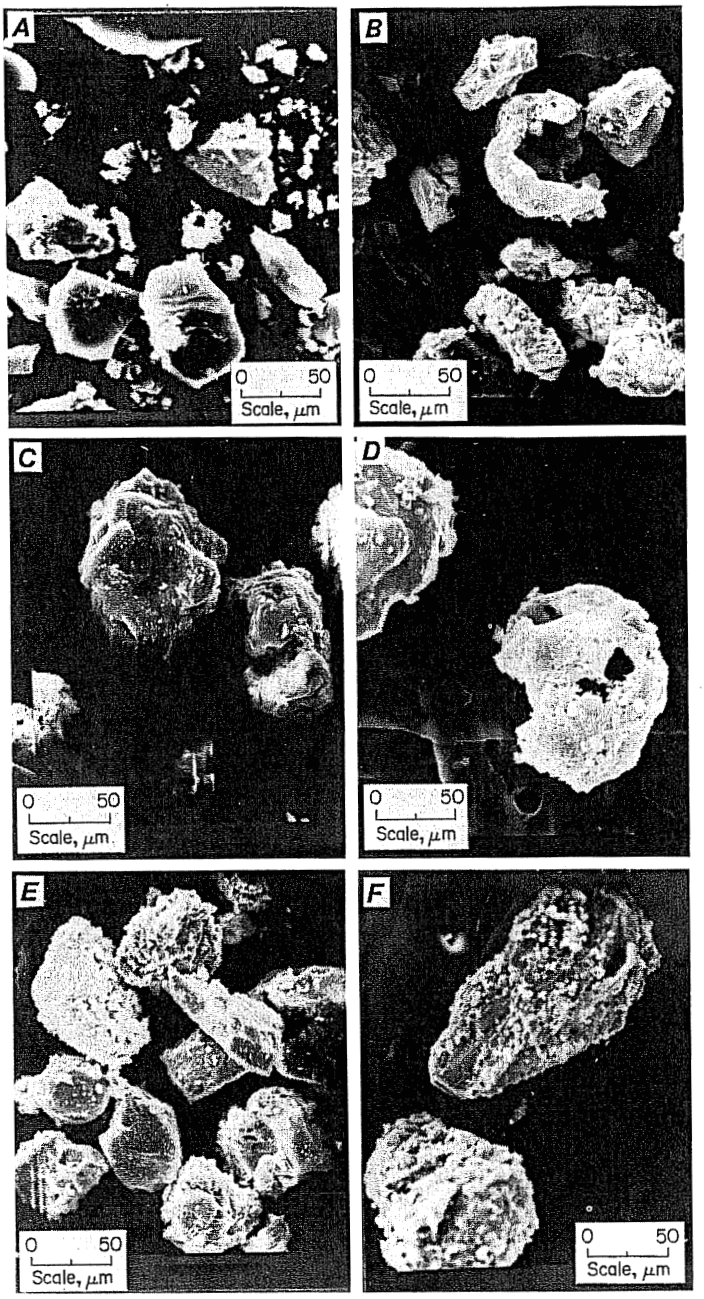

FIGURE 9 Micrographs of dust collected with sampling device during the explosion test LLEM-110.

DUST EXPLOSION MODELS

The coal dust made airborne by the turbulent pressure wave or shock front formed from the methane-air explosion is subject to a high heat flux from the radiation and hot gases in the rapidly approaching flame front. The coal particles heat up rapidly

TABLE II
Average gas composition (dry basis) of 6 runs with 35% PPC/65% Rock Dust at 200 g/m^3 nominal PPC concentration

Sampling	Percent, %										
	N_2	Ar	O_2	CO_2	CO	H_2	CH_4	C_2H_2	C_2H_4	C_2H_6	C_3H_6
Standard Air	78.08	0.936	20.95	0.032	0	0	0	0	0	0	0
Before flame	78.07	0.933	20.77	0.087	0.0024	0	0.0016	0	0	0	0
σ_m, ±	0.06	0.002	0.10	0.016	0.0012	0	0.0004	0	0	0	0
In flame	74.82	0.896	0.51	15.95	5.59	1.77	0.232	0.043	0.025	0.0013	0.0014
σ_m, ±	0.37	0.004	0.06	0.52	0.47	0.68	0.035	0.006	0.005	0.0003	0.0003

Note: The error limits are the standard deviation of the mean values, $\sigma_m = \sigma/\sqrt{n}$.

as the thermal wave progresses inward. First the adsorbed low weight species are desorbed from the pores, followed by thermal degradation of the polymeric material composing the bulk of the coal. The surface of the bituminous coal particle softens, becomes plastic and "skin-like." The volatiles produced form bubbles under this skin, and vent intermittently as the vapor pressure exceeds the tensile strength of the film. The particles so transformed are surrounded by a vapor halo. The halo also contains soot formed from the polymerization of some reactive unsaturated species. Oxygen diffusing in these hot vapors causes ignition. The burning halo atmosphere surrounding the particles releases heat energy to advance the flame front and engage coal particles nearby and further down stream. The mass loss of these particles is appreciably greater than the loss from a bed of particles placed in a closed crucible in a furnace, which is the standard volatility measurement procedure (ASTM D3175). In the latter case, there is both slow particle heat up and ample opportunity for condensation and polymerization of the vapors. Thus, the mass loss observed for a separated small array of Pittsburgh seam coal particles having diameters $\leqslant 100$ micrometers and subject to very rapid heating by a strong CO_2 laser flux of 100 or 200 W/cm^2 is about 50%, whereas it is only 37% in the ASTM procedure. For Pocahontas coal, the discrepancy is more striking. The ASTM volatility is only about 18%, whereas it is 33% with the laser technique. The laser flux used is roughly comparable to the heat flux in a well-developed explosion, taking into account the undirectional heating by the laser beam and the heat loses to both the cold sample substrate and the cold ambient gas (Cashdollar *et al.*, 1988).

There is some controversy in the literature over the possible involvement of heterogeneous burning of the charred coal particles in the explosion process. We can consider the two extremes; either char burning does not occur, or it occurs readily. In the former case, we may consider the coal to consist of a reactive volatile portion and an inert char. In the latter case, the entire coal reacts. Even here, the questions remains, "Does the char burning occur at a rate which can affect flame propagation?"

In coal dust explosions conducted in a 20-L laboratory chamber (Cashdollar *et al.*, 1985), only the volatiles appear to contribute significantly to flame propagation, and the char in fact, appears to act as a thermal inertant. The greater turbulence and flame residence time in a mine explosion, however, can lead to some char involvement. We will therefore consider both possibilities. Typical proximate and ultimate analyses of Pittsburgh and Pocahontas seam coals are given in Table III together with the ultimate analysis of their "fixed carbon," or char fractions. Empirical formulas of the

TABLE III
Proximate and ultimate analysis of Pittsburgh and Pocahontas seam coal and their components

Coal Seam	Proximate analysis (mass pct - as received)				Elements (mass pct - moisture ash free basis)				
	Volatiles	Fixed Carbon	Ash	Moisture	C	H	O	N	S
Pittsburgh									
Coal	37.9	54.5	6.6	0.94	82.67	5.62	8.74	1.79	1.18
0.50 Char					95.05	0.76	1.26	1.85	1.08
0.50 Volatiles					70.30	10.48	16.22	1.73	1.28
Pocahontas									
Coal	18.82	75.40	5.40	0.38	88.85	4.50	4.56	1.17	0.92
0.67 Char					96.70	0.93	0.36	1.14	0.87
0.33 Volatiles					73.14	11.64	12.96	1.23	1.02

coals and chars are derived and heats of formation, ΔH_f, are calculated based on the stoichiometric reactions and the experimental heats of combustion (moisture, ash-free basis). Taking the volatile fractions to be 0.50 and 0.33 for Pittsburgh and Pocahontas, respectively, one can deduce their elemental compositions heats of formation, and empirical formulas. The heats of formation of the volatiles are derived, as above, from deduced heats of combustion, ΔH_c, based on energy conservation. The formulas, ΔH_c, and ΔH_f for Pittsburgh and Pocahontas coals, and their components are given in Table IV. A prior analyses (Conti *et al.*, 1988) of Pittsburgh seam coal and volatiles gave $CH_{0.808}O_{0.082}N_{0.017}S_{0.006}$ and $CH_{1.64}O_{0.15}N_{0.015}S_{0.006}$.

In view of the uncertainties in the analyses and the "true" volatilities, one can simplify the formulas and heats of formation as shown in Table V. The heats of formation listed are somewhat arbitrary but have only a small effect on calculated flame temperature and product concentrations. The values chosen for the volatiles model give a reasonable limiting flame temperature (1400 K) for Pittsburgh seam coal dust explosions conducted in a laboratory chamber. The $CaCO_3$ component of the rock-dust/coal-dust mixtures is treated either as chemically inert or fully reactive at or above the decomposition temperature of 1170 K.

Thermodynamic calculations of the adiabatic flame temperature and product

TABLE IV
Formula and energy for Pittsburgh and Pocahontas seam coal and their components

Coal Seam	Empirical Formula	Combustion Heat (MAF) (cal/g)	Heat of Formation (cal/mol)
Pittsburgh			
Coal	$CH_{0.810}O_{0.079}N_{0.019}S_{0.0053}$	−8260	−2080
Char	$CH_{0.095}O_{0.010}N_{0.017}S_{0.0043}$	−7850	+1590
Volatiles	$CH_{1.777}O_{0.173}N_{0.021}S_{0.0068}$	−8670	−7080
Pocahontas			
Coal	$CH_{0.6036}O_{0.0385}N_{0.0113}S_{0.0039}$	−8640	+1820
Char	$CH_{0.1146}O_{0.0028}N_{0.0101}S_{0.0034}$	−8100	+2350
Volatiles	$CH_{1.897}O_{0.133}N_{0.0144}S_{0.0052}$	−9720	+ 407

TABLE V
Simplified Empirical Formulae and Heats of Formation (cal/mol).

	Whole Coal	Volatiles	Char
Pittsburgh Coal	$CH_{0.8}O_{0.08}$, $\Delta H°_f = 0$	$CH_{1.7}O_{0.15}$, $\Delta H°_f = -5000$	"C", $\Delta H°_f = 0$
Pocahontas Coal	$CH_{0.6}O_{0.04}$, $\Delta H°_f = 0$	$CH_{1.9}O_{0.13}$, $\Delta H°_f = 0$	"C", $\Delta H°_f = 0$

concentrations for methane and coal dust explosions were performed on a VAX 11/780 computer using the CEC-80 fortran code for complex equilibria calculations developed at the NASA-Lewis Research Center (Gordon and McBride, 1976). This program uses data taken primarily from the JANAF compilations of enthalpy, free energy, and other thermodynamic properties as a function of temperature (JANAF, 1985). The free energy of the system is minimized considering all possible species and concentrations derivable from the reactants within the constraint of conservation of energy and atoms. The enthalpy of this product mixture as a function of temperature then determines the final temperature. The pressure in a constant volume calculation is determined from the temperature and number of moles of gas by the ideal gas law. The temperatures, pressure, and concentrations are assumed to be uniform throughout the volume.

RESULTS AND ANALYSIS

The samples obtained from the gas zone in two experiments showed the high temperature combustion products expected from the measured initial methane concentrations of 10.63 ± 0.02 and $10.45 \pm 0.24\%$ in air that was measured by conventional sampling and analysis. In fact, the combustion product compositions corresponded to calculated starting methane concentrations of 10.84 ± 0.43 and $10.73 \pm 0.36\%$, respectively. The richer mixture gave the following dry gas composition: $N_2 + Ar = 82.46 \pm 0.22\%$, $O_2 = 0.96 \pm 0.47\%$, $CO_2 = 8.18 \pm 0.36\%$, $CO = 4.10 \pm 0.25\%$, $H_2 = 3.95 \pm 0.33\%$, $CH_4 = 0.237 \pm 0.135\%$ and a total of $0.0360 \pm 0.0180\%$ higher hydrocarbons. Of these, all but the methane and higher hydrocarbons are the expected concentrations of the flame temperature reaction products. The hydrocarbons detected can be attributed to background emission from desorbed gases in the mine. The significant concentrations of CO and H_2 (4% each) predicted and measured is understandable in view of the high adiabatic flame temperature calculated for these mixtures (2180 K) which favors the formation of diatomic and monatomic species.

The small concentration of free radicals such as OH, H, and O that were generated at these temperatures are too reactive to be detected by the rapid sampling technique. They simply recombine on the cold surfaces of the sampling probe needle and glass vial. The sampling, however, leads to a cooling rate which is, apparently, fast enough to inhibit other reactions, as evidenced by the agreement of the sampled burned gas composition with the flame calculation. The flame temperature composition is thus "frozen" by the sampling technique, which is a decided advantage.

In the experiments using low nominal concentrations of Pittsburgh seam coal dust (50–70 g/m^3), the average concentrations found were as follows: $N_2 + Ar = 80.64 \pm 0.55\%$, $O_2 = 6.75 \pm 0.45\%$, $CO_2 = 12.4 \pm 0.1\%$, and $CO = 0.20 \pm 0.14\%$. The concentrations were best matched by a calculated coal concentration of $75 \pm 7\ g/m^3$ for the reactive coal model, or $160 \pm 16\ g/m^3$ for the 50 volatilities, 50% inert char model. The same results were obtained on comparing

the 1930 $\pm$ 20 K peak temperature of the incandescent solids measured by a 3-wavelength near IR pyrometer (Cashdollar and Hertzberg, 1982 and 1983) stationed in the dust zone, with the results of the calculation. The agreement between the particle temperatures and gas concentrations suggest that the particle temperatures are close to that of the gas, and may be a measure of the temperature of submicron soot particles. The 6-wavelength pryometer (Cashdollar and Hertzberg, 1982 and 1983) should give a better average value of particle and gas temperatures and it would be more desirable, although more difficult for mine use. The 0–50% excess in calculated coal concentration over the nominal value in the reactive coal model is easily rationalized in terms of a non-uniform dust dispersion. That is, dust falling from the roof shelves will tend to produce a greater concentration in the upper region. The 200–300% excess concentration predicted by the volatiles model is more difficult to rationalize.

Particle temperature of 1910 K were also previously measured in mine explosions of fine Pocahontas coal particles at a nominal concentration of 40–50 g/m^3, that were dispersed and ignited as above, and compared with the adiabatic equilibrium predictions of the reactive and volatiles models for this coal. The reactive coal model gave a matching coal concentration of 70 g/m^3, while the 33% volatiles model predicted a concentration of 235 g/m^3. The latter concentration is 400–600% in excess of the nominal value and appears to be unrealistic. Based on these 3-wavelength pyrometer measurements, we may conclude that either char burning occurs in a mine explosion or that we have underestimated the true volatile yield. It should be noted, however, that the pyrometers in these experiments had not been calibrated, at that time, against a black-body source, and thus have an unknown accuracy.

A similar conclusion is reached in analyzing the gas concentration and particle temperatures in entrained mixtures of 35% PPC and 65% rock dust. The average dry gas composition is: $N_2 + Ar = 76.0 \pm 1.5\%$, $O_2 = 0.84 \pm 0.54\%$, $CO_2 = 16.2 \pm 1.8\%$, $CO = 5.4 \pm 2.0\%$, $H_2 = 1.7 \pm 0.7\%$. Using the reactive coal model and a chemically inert $CaCO_3$, the above concentrations are best matched by a 125 g/m^3 PPC concentration. This calculated value is 40% below the nominal 200 g/m^3 concentration. However, half of the dust in the PPC-Rock dust mixture was spread on the floor and may not have been lifted efficiently into the flame zone by the prior methane explosion. The measured temperature of 1810 $\pm$ 75 K is similarly fitted best by a 155 g/m^3 PPC concentration using the reactive coal—unreactive rock dust model. The corresponding reactive $CaCO_3$ model gives 125 and 130 g/m^3 as the best matching PPC concentrations for the experimental gas concentrations and temperatures, respectively. The 50% volatiles model gives 230 g/m^3 as the best matching PPC concentration. The best match to the experimental temperature was 200 g/m^3 PPC, which is the nominal value, for the unreactive $CaCO_3$. With reactive $CaCO_3$ the calculated temperatures are too low. Thus, either the 50% volatiles model with inert $CaCO_3$ or the reactive coal models account for the mine results. For 35% Pochahontas—65% $CaCo_3$ mixtures with a nominal coal concentration of 200 g/m^3 the previously measured 3-wavelength pyrometer temperature of 1900 K could however, be matched only by the reactive coal models which give 115 and 135 g/m^3 for the reactive and inert $CaCO_3$ models, respectively. Again, however, we must note the absence of a current calibration of the pyrometer, which mitigates against drawing firm conclusions based solely on temperature measurements.

CONCLUSIONS

Immediately prior to flame arrival, the background gas is virtually that of standard air with few particles showing signs of tar, volatiles or char formation. Gas samples

taken entirely in the flame zone consist of pyrolysis and combustion products with very little residual oxygen. The particles show signs of extensive pyrolysis and charring. The correlation between the experimental values of the gas composition and the particle temperatures with that calculated for models consisting of reactive Pittsburgh or Pocahontas coals is suggestive, but not conclusive evidence of char burning in mine explosions. These experimental results, demonstrate the utility of the high-speed gas and dust sampling systems, in analyzing large scale explosions.

The system can be further upgraded by interfacing a microprocessor or computer to enhance timing capabilities and eliminate the relay control package. For example, data from a set of flame sensors upstream of the sampling system could be used by a microprocessor to calculate the expected time of flame arrival and thereby insure sampling of the flame zone or even its leading edge. A more definitive test of the reactive coal and $CaCO_3$ vs inert char and $CaCO_3$ models could then be obtained.

REFERENCES

Cashdollar, K.L., Liebman, I., and Conti, R.S. (1981). Three Bureau of Mines Optical Dust Probes. U.S. Bureau of Mines RI 8542, 26.

Cashdollar, K.L. and Hertzberg, M. (1982). Infrared Pyrometers For Measuring Dust Explosion Temperatures. *Optical Engineering,* **21,** 82.

Cashdollar, K.L. and Hertzberg, M. (1983). Infrared Temperatures of Coal Dust Explosions. *Combustion and Flame,* **51,** 23.

Cashdollar, K.L. and Hertzberg, M. (1985). 20-L Explosibility Test Chamber for Dusts and Gases. *Review Scientific Instruments,* **56,** 596.

Cashdollar, K.L., Hertzberg, M., and Zlochower, I.A. (1988). Effect of Volatility on Dust Flammability Limits for Coals, Gilsonite, and Polyethylene. Twenty-second Symposium (International) on Combustion, The Combustion Institute, Pittsburgh, pp. 1757–1765.

Conti, R.S., Cashdollar, K.L., and Liebman, I. (1982). Improved Optical Probe for Monitoring Dust Explosion. *Review of Scientific Instruments,* **53,** 311.

Conti, R.S., Hertzberg, M., Duda, F.T., and Cashdollar, K.L. (1983). Rapid-Sampling Systems for Dusts and Gases. *Review of Scientific Instruments,* **54,** 104.

Conti, R.S., Zlochower, I.A., and Sapko, M.J. (1988). Rapid (Grab) Sampling During Full-Scale Explosions—Microscopic and Analytical Evaluation. U.S. Bureau of Mines RI 9192, 17.

Gordon, S. and McBride, B.J. (1976). Computer Program For Calculation of Complex Chemical Equilibrium Composition. National Aeronauatics and Space Administration, SP-273, 251.

JANAF, Thermochemical Tables, 3rd Edition, M.W. Chase Jr., et al, Eds. (1985). *Journal of Physical and Chemical Reference Data, Vol* **14,** *Suppl.* 1.

Liebman, I., Duda, F., and Conti, R.S. (1979a). Sensor Trigger Device for Explosion Barrier. *Review Scientific Instruments,* **50,** 1441.

Liebman, I., Duda, F., and Conti, R.S. (1979b). Sensor Trigger Device for Explosion Barrier. U.S. Pat 4, 173, 140.

Mattes, R.H., Bacho, A., and Wade, L.W. (1983). Lake Lynn Description: Construction, Physical Description, and Capability. U.S. Bureau of Mines IC 8911, 40.

Ng, D.L., Cashdollar, K.L., Hertzberg, M., and Lazzara, C.P. (1983). Electron Microscopy Studies of Explosions and Fire Residues. U.S. Bureau of Mines IC 8936, 63.

Richmond, J.K. and Liebman, I. (1975). A Physical Description of Coal Mine Explosions. *Fifteenth Symposium (International) on Combustion,* The Combustion Institute, Pittsburgh, pp. 115–126.

Richmond, J.K., Liebman, I., Bruszak, A.E., and Miller, L.F. (1978). A Physical Description of Coal Mine Explosions. Part II. Seventeenth Symposium (International) on Combustion, The Combustion Institute, Pittsburgh, pp. 1257–1268.

Sapko, M.J., Weiss, E.S., and Watson, R.W. (1987). Size Scaling of Gas Explosions: Bruceton Experimental Mine Versus the Lake Lynn Mine. U.S. Bureau of Mines RI 9136, 23.

Weiss, E.S., Greninger, N., and Sapko, M.J. (1988). Recent Results of Dust Explosion Studies at the Lake Lynn Experimental Mine. Presented at the *Twenty-third Conference (International) Safety in Mines Research Instiutes,* Washington, DC, pp. 843–854.